Lattice Boltzmann method on irregular meshes

Gongwen Peng, Haowen Xi, and Comer Duncan

Department of Physics and Astronomy, Bowling Green State University, Bowling Green, Ohio 43403

So-Hsiang Chou

Department of Mathematics and Statistics, Bowling Green State University, Bowling Green, Ohio 43403

A finite-volume scheme for the lattice Boltzmann method (FVLBM) is described. The scheme uses a finite-volume formulation based on triangular elements in two dimensions and is implemented assuming that velocity space is isotropically discretized at each node in position space. The accuracy of the finite-volume scheme is numerically demonstrated by comparing the computed macroscopic velocity field with the exact solution of the Navier-Stokes equations for the flow of an incompressible fluid between two relatively rotating cylinders. The FVLBM scheme is applicable to irregular two-dimensional regions which contain both exterior and interior boundaries of arbitrary shape. Thus, the range of applicability of systems to which the FVLBM may be applied is seen to be significantly extended. [S1063-651X(98)51810-7]

PACS number(s): 47.10.+g, 47.11.+j, 05.20.Dd

Recently the lattice Boltzmann method (LBM) has been demonstrated to be an effective simulation method for fluid flow and other types of complex physical systems [1–4]. Unlike conventional computational fluid dynamics (CFD), which solves the macroscopic Navier–Stokes equations, the LBM is based on the mesoscopic kinetic equation for the single particle distribution function. By incorporating the essential physics of microscopic or mesoscopic processes, the LBM is constructed so that the macroscopic properties obey the desired macroscopic equations. The obvious advantages are the simplicity of programming, the natural parallelism of the algorithm, and the capability of incorporating complex microscopic interactions.

However, compared to the state-of-the-art CFD techniques, the LBM still suffers some limitations. One of these is that the LBM is constructed on a special class of uniform and regular spatial lattices. Historically, the LBM was developed from the lattice gas automaton (LGA) [5] model where the concept prevails of particles jumping from one site to the other on a regular lattice. The particle distribution function in the LBM was interpreted as the floating-number counterpart of the Boolean particle occupation in the LGA. The limitation of using uniform lattices in the LBM is particularly severe in many applications where the complex geometry of internal and external boundaries cannot be well fitted by regular lattices. During the past few years, several researchers were motivated by such considerations to extend the applicability of the LBM to irregular lattices. Succi and co-workers [6] have proposed a finite-volume formulation of the lattice Boltzmann equation (LBE). The basic idea is to start from the differential form of the LBE and apply the Gauss's theorem to a set of macro-cells covering the spatial domain. For each cell, a volume-averaged ''coarse-grain'' particle distribution is defined and by using either piecewise constant or piecewise linear interpolation schemes they obtain equations for the ''coarse-grain'' distribution functions. In the model of He, Luo, and Dembo [7] for an arbitrary rectangular mesh, collisions still take place on the grid points. After a collision, the density distributions move along their respective velocities' directions to points that may or may not be on grid points. An interpolation step is then introduced to determine the density distributions at the grid points for the next time step, and the above procedures are repeated.

However, the above-mentioned approaches of using irregular meshes are not satisfactory in the sense that the topology of the meshes used in the proposed models is not arbitrary. For example, in the 2D simulations of previous works, each mesh grid point is connected to four other points [6,7] in association with nine discrete velocities. This is still far from the modern CFD methods, which are generally capable of accommodating fairly complex spatial meshes. To overcome this shortcoming, in this Rapid Communication we describe a computational scheme based on arbitrary two-dimensional triangular meshes from the point of view of modern finite-volume methods [8,9]. The scheme we report in this paper is applicable to irregular meshes with arbitrary connectivity. While our methods follow from an application of finite-volume methods to the LBE, they still keep much of the simplicity of the conventional LBM. As an illustration of the power of these methods, we will demonstrate that this scheme works remarkably well when applied to the flow of an incompressible fluid between two relatively rotating cylinders.

Our starting point is the LBE. Recently, it was shown [10] that the LBM can be directly derived from the Boltzmann equation by discretization of phase space. Specific discretizations of the LBE on regular lattices along with some special assumptions concerning the length, time, and characteristic velocities give the commonly used LBM models in which the spatial and velocity space lattices are closely coupled. More general finite difference discretizations of the LBE were studied in Ref. [11] and have been extended to efficient parallel schemes [12]. The flexibility gained in unlocking the spatial and velocity lattices from each other provides us with an important degree of freedom in designing our finite-volume scheme.

After discretizing the velocity space, the LBE reads as follows:

$$\frac{\partial f_i}{\partial t} + \mathbf{v}_i \cdot \boldsymbol{\nabla} f_i = \Omega_i, \tag{1}$$

where f_i is the particle distribution function associated with motion along the ith direction in velocity space, $\mathbf{v}_i$ the velocity in the ith direction, $i = 1,2,...,m$ with m the number of different velocities in the model, and Ω_i is the collision operator. Many workers have used the lattice Bhatnagar-Gross-Krook (BGK) model [13], or the single-time relaxation approximation for the collision operator,

$$\Omega_i = -\frac{1}{\tau}(f_i - f_i^{eq}), \tag{2}$$

where f_i^{eq} is the local equilibrium distribution and τ is the relaxation time.

In the LBM, only a small set of discrete velocities are used to approximate the Boltzmann kinetics of the continuum velocity. In the original formulations of the LBM it was understood that the discretization of momentum space is coupled to that of position space. For example, one model utilized by a number of workers used nine discrete velocities in association with the square lattice in position space in two dimensions. For a triangular spatial lattice seven velocity space directions were used and they were closely tied to the triangular spatial lattice. But as emphasized in Refs. [14, 7, 11, this coupling is not necessary and both discretizations can be done independently. Here we will completely decouple these two discretizations by choosing the nine velocities as in the nine-bit model for the velocity discretization and arbitrary triangular meshes for the spatial discretization.

The nine discrete velocities are defined by $\mathbf{v}_i = (0,0)$ for $i = 0$, $(\cos[(i-1)\pi/2], \sin[(i-1)\pi/2])$ for $i = 1,2,3,4$, and $(\sqrt{2}(\cos[(i-5)\pi/2 + \pi/4], \sin[(i-5)\pi/2 + \pi/4])$ for $i = 5,6,7,8$. The equilibrium distribution f_i^{eq} is given by

$$f_i^{eq} = w_i \rho [1 + \tfrac{3}{2}(\mathbf{v}_i \cdot \mathbf{u}) + \tfrac{9}{2}(\mathbf{v}_i \cdot \mathbf{u})^2 - \tfrac{3}{2}|\mathbf{u}|^2], \tag{3}$$

where $\rho = \Sigma_i f_i$ and $\rho\mathbf{u} = \Sigma_i f_i \mathbf{v}_i$ are the macroscopic mass density and momentum density respectively, and w_i equals $\frac{4}{9}$ for $i = 0$, $\frac{1}{9}$ for $i = 1, 2, 3, 4$, and $\frac{1}{36}$ for $i = 5,6,7,8$.

In the scheme reported here we use two-dimensional triangular meshes to illustrate how our finite-volume scheme is constructed. The extension to three dimensions and to other types of meshes is straightforward. For example, in a 2D simulation one can easily apply a similar formulation which uses irregular quadrilateral meshes whose node connectivity can be much more complex than the nonuniform rectangular meshes used in the previous studies [6,7].

In Fig. 1 we show the generic situation in which triangular elements surround an interior node of the mesh. Here we report a finite-volume method of the cell-vertex type. In this type of formulation, the f_i's at the nodes are the unknowns. When we need to calculate the f_i's at non-node positions, these values would be interpolated from the f_i's at the nodes
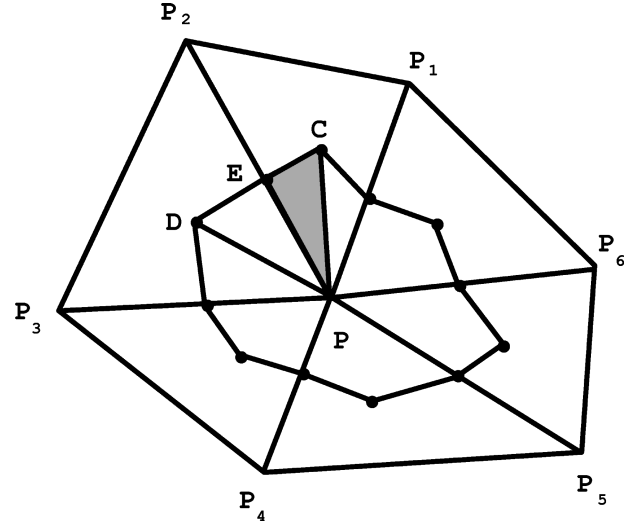

FIG. 1. Diagram of finite elements sharing one common node. Here $P, P_1, P_2, ..., P_6$ stand for the mesh grid point. CE and ED are two boundary edges of the control volume (polygon) over which integration of the LBE is performed.

using standard interpolation procedures depending on the element types used. For example, linear and "bilinear" interpolations would be applied to the triangular and quadrilateral elements, respectively.

We choose the control volume to be the polygon surrounding the node P, as shown in Fig. 1. Two sides of the polygon, CE and ED, are labeled in the figure. Here E is the midpoint of edge PP_2, C is the geometric center of element PP_1P_2 with coordinates $\mathbf{x}_E$ and $\mathbf{x}_C$, respectively. Likewise, D is the center of element PP_2P_3. The integration volume consists of triangles PCE, PED, etc. taken in counterclockwise order. In the following we focus on the integration over the triangle PCE. Similar integrations would be done over all such triangles centered on P and the results summed.

The integration of the first term in Eq. (1) is approximated as

$$\int_{PCE} \frac{\partial f_i}{\partial t} d\sigma = \frac{\partial f_i(P)}{\partial t} A_{PCE}, \tag{4}$$

where A_{PCE} is the area of triangle PCE and $f_i(P)$ is the f_i value at node P. In what follows, the node index is given in parentheses following the f_i values. In the above equation, we have made an approximation that f_i is constant over the triangle PCE to prevent us from having to solve a set of equations if f_i's were assumed linear. This kind of "lumping" is a commonly used practice in the finite-volume methods [9].

Integration of the second term of Eq. (1) will give fluxes through the three edges PC, CE and EP. Since we will sum over all the triangles like PCE, PED, the net flux through internal edges (e.g., PC, PE) will cancel out. Therefore, we will omit the contribution from the internal edges. On the assumption of linearity of the f_i's for the triangular elements, the flux is given by

$$\int_{PCE} \mathbf{v}_i \cdot \nabla f_i d\sigma = \mathbf{v}_i \cdot \int_{CE} f_i d\mathbf{l} + I_s = \mathbf{v}_i \cdot \mathbf{n}_{CE} l_{CE}[f_i(C)$$

$$+ f_i(E)]/2 + I_s, \qquad (5)$$

where $\mathbf{n}_{CE}$ is the unit vector normal to the edge CE, l_{CE} is the length of CE, and I_s is the fluxes from the internal edges.

The integration over the collision term of Eq. (1) [i.e., Eq. (2)] results in the following formula, assuming the linearity of f_i and f_i^{eq} over the triangular element:

$$-\int_{PCE} \frac{1}{\tau}(f_i - f_i^{eq})d\sigma = -\frac{A_{PCE}}{\tau}\{[f_i(P) - f_i^{eq}(P)] + [f_i(C)$$

$$-f_i^{eq}(C)] + [f_i(E) - f_i^{eq}(E)]\}/3, \qquad (6)$$

where $f_i(C)$ and $f_i(E)$ and their corresponding equilibrium particle distribution functions are the values of these variables at C and E, respectively. These may be easily obtained by interpolation from the three nodes at element PP_1P_2.

With these results, the integration of Eq. (1) over the triangle PCE is complete. The integration over the whole control volume is just the sum of contributions from all these terms over different triangles such as PCE, PED, etc. Therefore, f_i at node P is updated as follows:

$$f_i(P, t+dt) = f_i(P, t) + \frac{dt}{A_P}\left(\sum_{around \; P} \Phi_{collisions}\right.$$

$$\left. - \sum_{around \; P} \Phi_{fluxes}\right), \qquad (7)$$

where A_P is the total area of the control volume around node P, $\Phi_{collisions}$ and Φ_{fluxes} refer respectively to the finite-volume-integrated contributions from the collision term and fluxes. The summation is over different triangles PCE, PED, etc. associated with the node P.

To demonstrate the flexibility of the above scheme we present an example of simulation of an incompressible fluid flow between two coaxial cylinders. Figure 2 gives an example of an irregular mesh adapted to the two cylinder problem. Note that for any irregular boundary geometry, it is always possible to cover the domain using triangular elements, as is shown here for the cylinders.

For the initial conditions we take the macroscopic velocity field between the cylinders to be zero. Then the outer cylinder suddenly starts to rotate with a constant angular velocity Ω while the inner cylinder is kept at rest. Note that this particular problem possesses high symmetry so that an appropriate finite difference scheme adapted to cylindrical coordinates can also handle it [11]. The FVLBM scheme reported here needs no assumptions of symmetry and thus is capable of handling a wide variety of geometries without modification. In the finite-volume scheme, the update of the f_i's at boundary nodes is similar to that for interior nodes except at the boundary the corresponding covolumes are half-covolumes.

In Fig. 3 we show the stationary velocity profile for the angular component of the macroscopic velocity which results from our computations compared with the theoretical solu-
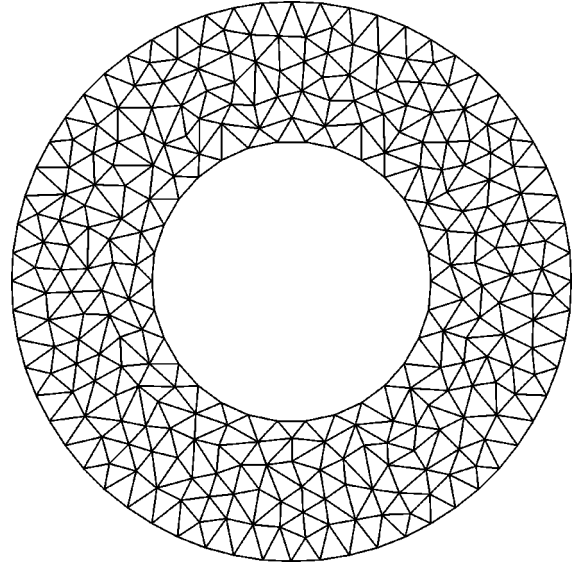

FIG. 2. An irregular mesh between two coaxial cylinders.

tion of the Navier-Stokes equation [15]. Here we have taken the radii of the two cylinders to be $R_1 = 50$ and $R_2 = 100$ and the angular velocity of the outer cylinder is $\Omega = 0.0005$ rad per unit time. The effective mesh spacing of our triangular mesh is of the order of 1 and the relaxation time τ is taken to be 0.1. The average density ρ_0 is set to be 1.0. During the simulations we observed the density to stay very close to ρ_0, thus confirming that the evolution maintains the incompressibility of the fluid between the relatively rotating cylinders. We evolved the system for 3×10^6 time steps with $dt = 0.01$ and observed it to monotonically approach the exact stationary solution for the velocity profile. The time step dt was well within the effective Courant limit throughout the simulations. The CFL condition in the current finite volume scheme is found to be of the form $v_i dtc/h \leq 1$, where h is a minimum length scale of the control volume and c is a con-
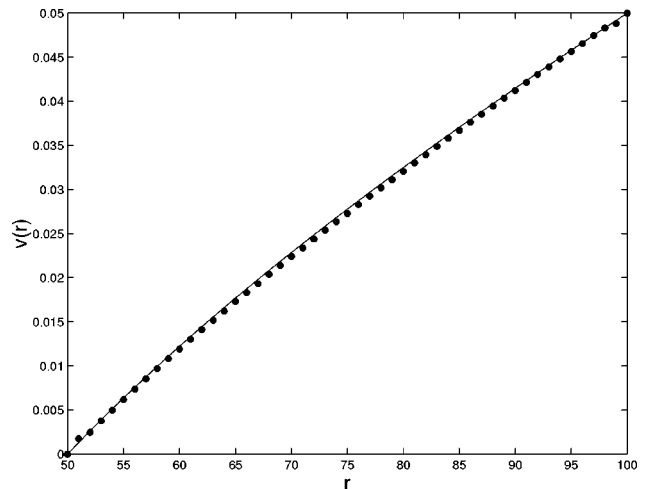

FIG. 3. The steady state velocity profile of flow between two coaxial cylinders (points), compared with the theoretic solution (curve) of the Navier-Stokes equation $v(r) = ar - b/r$ with $a = \frac{2}{3} \times 10^{-3}$ and $b = \frac{5}{3}$. Here each point is the average of the angular velocities at the nodes in a circular layer between $r - 1/2$ and $r + 1/2$ with r integers.

stant depending on the shape of the control volume. From Fig. 3 one can see that the agreement with the theoretical results is quite good. To gain a quantitative measure of the accuracy, we have computed the L_1 norm of the difference between the computed and exact velocity profiles. The global error was found to be 1.0%, indicating that our computed velocity profile agrees well with the exact profile.

It is interesting to make a comparison between the above scheme and the finite-volume scheme of Succi and co-workers [6]. First, their model is a cell centered finite-volume method while our scheme is cell-vertex. In the model of Succi and co-workers [6], the ''coarse grain'' density distribution is the unknown for each macro-cell. Second, in their model the piecewise constant extrapolation for the streaming operator causes serious problems of numerical diffusion. Even for the piecewise linear interpolation, numerical diffusion does not disappear. To minimize this numerical diffusion, a free parameter is then introduced and its value is to be adjusted for each problem on a case by case basis. Third, even for the meshes with the simple connectivity of a logically rectangular lattice, their empirical formulas for the streaming coefficients are very complex and one could imagine the practical difficulty of using irregular meshes with arbitrary connectivity.

By comparison, our scheme is based on the standard finite-volume methods. It involves minimum approximation and does not need to introduce any free parameters. We have not found numerical diffusion problems in our finite volume scheme. The formulation on which our model is based does not require a special mesh connectivity and is easy to apply to other kinds of meshes (such as quadrilateral elements in 2D and tetrahedral and hexahedral elements in 3D) by replacing the standard interpolation we used here for triangular elements with other standard interpolation procedures suitable for the relevant types of volumes.

We have found that the kinematic viscosity in our finite-volume scheme is equal to $\tau/3$ independent of various meshes we used and independent of mesh sizes. Since our scheme is based on the LBE, which is continuous in space and time, it is understandable that this $\tau/3$ relation coincides with that obtained directly from the continuous equations [11].

To conclude, we have proposed a finite-volume scheme for the LBM which is flexible and can be applied to unsteady, incompressible fluid flow in a wide variety of two-dimensional regions that contain arbitrarily shaped internal and external boundaries. This opens up the LBE methods to be applied to many interesting systems so far difficult to treat using the conventional LBM. Several applications as well as extensions to thermal problems are under investigation and will be reported elsewhere [16].

[1] *Lattice Gas Method for Partial Differential Equations*, edited by G. D. Doolen (Addison-Wesley, Redwood City, CA, 1990); *Lattice Gas Methods: Theory, Applications and Hardware*, edited by G. D. Doolen (MIT, Cambridge, MA, 1991).

[2] R. Benzi, S. Succi, and M. Vergassola, Phys. Rep. **222**, 145 (1992).

[3] J. Stat. Phys. **81**, 10 (1995), special issue on lattice-based models and related topics, edited by J. L. Lebowitz, S. A. Orszag, and Y. H. Qian.

[4] S. Chen and G. D. Doolen (unpublished).

[5] U. Frisch, B. Hasslacher, and Y. Pomeau, Phys. Rev. Lett. **56**, 1505 (1986).

[6] S. Succi, G. Amati, and R. Benzi, J. Stat. Phys. **81**, 5 (1995); F. Nannelli and S. Succi, *ibid.* **68**, 401 (1992); G. Amati, S. Succi, and R. Benzi, Fluid Dyn. Res. **19**, 289 (1997).

[7] X. He, L.-S. Luo, and M. Dembo, J. Comput. Phys. **129**, 357 (1996).

[8] K. W. Morton, *Numerical Solutions of Convection-Diffusion Problems* (Chapman & Hall, London, 1996).

[9] C. Hirsch, *Numerical Computation of Internal and External Flows: Fundamentals of Numerical Discretization* (Wiley, Chichester, 1988), Vol. I.

[10] X. He and L.-S. Luo, Phys. Rev. E **55**, R6333 (1997); **56**, 6811 (1997).

[11] N. Cao, S. Chen, S. Jin, and D. Martínez, Phys. Rev. E **55**, R21 (1997).

[12] Z. Weng and C. Duncan (unpublished).

[13] P. L. Bhatnagar, E. P. Gross, and M. Krook, Phys. Rev. **94**, 511 (1954).

[14] S. Chen, D. Martínez, and R. Mei, Phys. Fluids **8**, 2527 (1996).

[15] G. K. Batchelor, *An Introduction to Fluid Dynamics* (Cambridge University Press, Cambridge, England, 1967).

[16] G. Peng, H. Xi, C. Duncan, and S-H Chou (unpublished).